

Ultrafast charge generation in a semiconducting polymer studied with THz emission spectroscopyE. Hendry,^{1,*} M. Koeberg,¹ J. M. Schins,² L. D. A. Siebbeles,² and M. Bonn^{1,3}¹*Leiden Institute of Chemistry, Leiden University, P.O. Box 9502, 2300 RA Leiden, The Netherlands*²*Interfaculty Reactor Institute, Delft University of Technology, Mekelweg 15, 2629 JB Delft, The Netherlands*³*FOM Institute for Atomic and Molecular Physics, Kruislaan 407, 1098 SJ, Amsterdam, The Netherlands*

(Received 30 December 2003; revised manuscript received 16 April 2004; published 22 July 2004)

We study the ultrafast charge generation in a semiconducting polymer (MEH-PPV) by measuring the radiated THz field after photoexciting the biased polymer with a femtosecond visible pulse. The subpicosecond temporal characteristics of the emitted wave reflects the ultrafast photoconductivity dynamics and sets an upper limit for charge generation of 200 fs following photoexcitation, and reveals the dispersive nature of charge transport in MEH-PPV. A comparison of the fields radiated from MEH-PPV and the well-characterized model semiconductor system (GaAs) allows for an accurate estimate of the quantum efficiency for charge generation in the polymer, found to be less than 1%. Both observations are consistent with ultrafast charge generation in semiconducting polymers through hot exciton dissociation.

DOI: 10.1103/PhysRevB.70.033202

PACS number(s): 72.80.Le, 73.50.Gr, 73.61.Ph, 71.35.Aa

Semiconducting conjugated polymers have recently received much interest owing to their potential in technological applications, particularly in electronics.¹ Despite this fact, the fundamentals of the photoexcitation physics in these materials have remained controversial: there is ongoing debate whether a band structure description is appropriate to these materials.^{2,3} In this picture, interband excitations directly generate free charges, which may relax to lower energy bound states. This strongly contrasts the exciton model, in which molecular excitons are formed upon photoexcitation, so that secondary processes such as exciton-exciton annihilation⁴ or hot exciton dissociation^{5,6} are required to generate free charges.

Although the observation of significant photoconductivity⁷ demonstrates the presence of free charges, it is unclear whether carriers are generated directly on ultrafast time scales or produced on longer time scales through, for example, exciton-exciton annihilation. Unfortunately, conventional transient photoconductivity measurements^{8,9} lack the resolution to resolve the ultrafast excitation process. Using time-domain THz spectroscopy,¹⁰ we have recently shown that photoexcitation of the polymer poly(2-methoxy-5-(2'-ethyl-hexyloxy)-*p*-phenylene vinylene) (MEH-PPV) leads to the generation of charges within 300 fs.¹¹ Additional information about the time scale of charge carrier generation and nature of the transport can be obtained by probing the radiation dispersed by the accelerating charges.^{12,13} When changes in photocurrent occur on (sub) picosecond time scales, THz radiation is emitted. The shape of the THz pulse is determined by the rise and decay of the photocurrent, and thus provides a direct probe of the ultrafast transient photoconductivity. In this manner, information regarding the rate of charge carrier generation and time-dependent mobility can be obtained. This technique is ideally suited to the study of charge generation and cooling on sub-picosecond time scales, and has been successfully applied to study the photoexcitation dynamics in materials such as low-temperature grown GaAs.¹³ Previous measurements on semiconducting polymer systems have also proven useful,¹² but suffered

from a limited bandwidth so that subpicosecond processes could not be resolved.

In this report we employ THz emission spectroscopy to study the ultrafast charge generation in a semiconducting polymer (MEH-PPV). We set an upper limit for charge generation in MEH-PPV within the first 200 fs after photoexcitation. By comparing our results to a model system (GaAs) the quantum efficiency for charge generation in the polymer is found to be less than 1%—over two orders of magnitude lower than in GaAs. Both conclusions are consistent with charge generation through hot exciton dissociation.

The insulating GaAs crystal is $\langle 100 \rangle$ cut, produced by Wafer Technology, LTD. The $\sim 20 \mu\text{m}$ MEH-PPV films are prepared by drop casting from chloroform solution onto water free quartz plates, using dry polymer from Sigma Aldrich. Silver electrodes are placed directly on the GaAs crystal and copper electrodes are incorporated into the polymer film. In both cases, a static field of 10 kV/cm is applied. At such low field charge injection effects are negligible,¹⁴ and only photocurrent is observed. Photoexcitation is accomplished with 400 nm (3 eV) laser pulses with durations of 180 fs [full width at half maximum (FWHM)], allowing above band gap excitation of both GaAs and MEH-PPV [1.6 (Ref. 13), and 2.4 eV (Ref. 14), respectively]. A parabolic mirror is placed as close to the samples as possible to properly collect all radiated frequency components. The emitted THz pulse is detected in the far field through electro-optical sampling¹⁵ using 800 nm pulses (FWHM 180 fs) incident on a 1.2 mm $\langle 110 \rangle$ ZnTe crystal.

The measured THz fields $E_{\text{meas}}(t)$ emitted by the GaAs and MEH-PPV samples are shown in Figs. 1(a) and 1(b), for absorbed fluences¹⁶ of 10 and 225 $\mu\text{J}/\text{cm}^2$, respectively. For MEH-PPV, a higher fluence is required to obtain sufficient signal to noise, while for GaAs care must be taken to avoid detector saturation. Although the signal *amplitude* scales linearly with both the strength of the applied bias field and the photoexcitation intensity, the signal *shape* is independent of these experimental parameters. In both samples the THz pulse is radiated only when *both* the static field and excita-

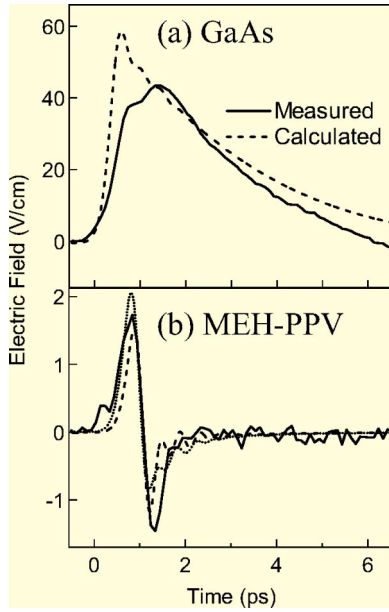


FIG. 1. Electric fields radiated from (a) GaAs, excited using $10 \mu\text{J}/\text{cm}^2$, 180 fs, 400 nm pulses, and (b) MEH-PPV, excited using the same pulses at $225 \mu\text{J}/\text{cm}^2$, both biased with an external field of 10 kV/cm. The broad positive peak in the generated field in (a) is due to a slow rise in photocurrent resulting from electron cooling effects. In (b), the sharp change in electric field direction suggests a peak in photoconductivity: the initial rise in photocurrent due to generation of carriers is offset by a rapid decrease in carrier mobility due to the finite conjugation length of the polymer backbone. The dashed lines show the response calculated using time dependent mobilities from Refs. 23 and 25, respectively, plotted in Fig. 2, assuming instantaneous generation of charges. The dotted line in (b) shows the corresponding pulse assuming charges generated by hot excitons with a dissociation rate of $(200 \text{ fs})^{-1}$ (Ref. 29).

tion pulses are present, ruling out optical rectification¹⁷ as a source of the signal. Despite the lower fluence, the pulse emitted from the GaAs sample is approximately 25 times larger than that from MEH-PPV. The wave forms are also very different in shape, with one main peak from the GaAs photocurrent, while the MEH-PPV sample gives approximately equal positive and negative peaks, indicating that the rise and fall of photocurrent in this sample occurs on a very similar time scale. Also, the GaAs signal is much broader, with a width ~ 3 ps, compared to < 1 ps for the polymer.

To model the data shown in Fig. 1, we note that the emitted THz in the far field $E(t)$ is proportional to the time derivative of the time-dependent current density.¹⁸ The current can be written as a convolution of the time-dependent carrier generation rate and the mobility $G(t)$ and $\mu(t)$, so that

$$E(t) \propto \frac{\partial}{\partial t} E_{\text{app}} \int_0^{+\infty} \mu(\tau) G(t - \tau) d\tau, \quad (1)$$

where E_{app} is the applied static field in the sample driving the current. To compare $E(t)$ to $E_{\text{meas}}(t)$, we have to account for the propagation of the field through the electro-optic sensor used in the experiments. The detected wave form $E_{\text{det}}(t)$ is related to $E(\omega)$, the Fourier transform of $E(t)$, through the

detector response function $f(\omega)$, such that $E_{\text{det}}(\omega) = f(\omega)E(\omega)$.¹⁵ Gallot and Grischkowsky¹⁵ have analyzed this distortion of THz pulses during electro-optic sampling to be

$$f(\omega) = \left[\int_{-\infty}^{+\infty} E_{\text{opt}}^*(\omega') E_{\text{opt}}(\omega' - \omega) d\omega' \right] \times \chi_{\text{dif}}^{(2)}(\omega) \times \frac{\exp\left(\frac{i\omega l}{c} \Delta n(\omega)\right) - 1}{\frac{i\omega l}{c} \Delta n(\omega)}. \quad (2)$$

The first term is the frequency domain autocorrelation of the 800 nm detection pulse, described by a Gaussian FWHM 5.0 THz. The second term is the second order susceptibility for difference frequency generation at 800 nm.¹⁵ The final, and dominant, term describes the velocity matching of the 800 nm detection pulse and the THz frequency ω required for efficient detection in our ZnTe electro-optic sensor of length $l = 1.2$ mm, where $\Delta n(\omega) = \vec{n}_{\text{THz}}(\omega) - n_{800 \text{ nm}}^{\text{group}}$ with $\vec{n}_{\text{THz}}(\omega)$ the complex THz refractive index and $n_{800 \text{ nm}}^{\text{group}}$ the refractive index corresponding to the group velocity at 800 nm. We use the measured values of Gallot *et al.*¹⁹ for $\vec{n}_{\text{THz}}(\omega)$, while the group index at 800 nm in ZnTe has been evaluated by Bakker *et al.*²⁰ to be 3.24. Therefore by modeling $G(t)$ and $\mu(t)$ in Eq. (1), we can calculate $E(t)$ and propagate the wave form through our sensor, obtaining $E_{\text{det}}(t)$, to reproduce the data in Fig. 1.

As several dynamic processes may occur directly following photoexcitation, carrier properties on ultrafast time scales can be very different from the equilibrium behavior of a material. Hence it seems inappropriate to use steady state mobilities [~ 8000 and $\sim 10^{-5} \text{ cm}^2/\text{V s}$ for GaAs (Ref. 21) and MEH-PPV (Ref. 22), respectively] to describe $\mu(t)$ on subpicosecond time scales after excitation. In the case of GaAs, exciting at 400 nm (with 1.5 eV excess energy) results in photoelectrons having sufficient energy to undergo inter-valley scattering into the higher energy L and X valleys. However, the low mobility of electrons in these valleys mean the onset of photoconductivity is delayed, as it is determined by the dynamics of electrons scattering into the high mobility Γ valley. The resulting time-dependent mobility in GaAs $\mu(t)$ can be calculated using a kinetic model developed by Stantan and Bailey,²³ assuming asymptotic behavior at long times to the steady state electron mobility of $8000 \text{ cm}^2/\text{V s}$,²¹ as plotted in Fig. 2(a). Evolution of the hole response is ignored in this calculation since hole mobilities are over an order of magnitude lower.²⁴ Also plotted is the generation rate $G(t)$ given by the Gaussian intensity profile of the 400 nm excitation pulse. It is clear that the slow evolution of the THz field emitted from the sample in Fig. 1(a) arises from slow cooling of electrons and the resulting slow rise in $\mu(t)$, rather than a slow generation process. Indeed, we can reproduce the data in Fig. 1(a) quite well—the result is plotted as a dashed line in the figure—using Eqs. (1) and (2). It should be noted that the only adjustable parameter is the amplitude of $G(t)$.

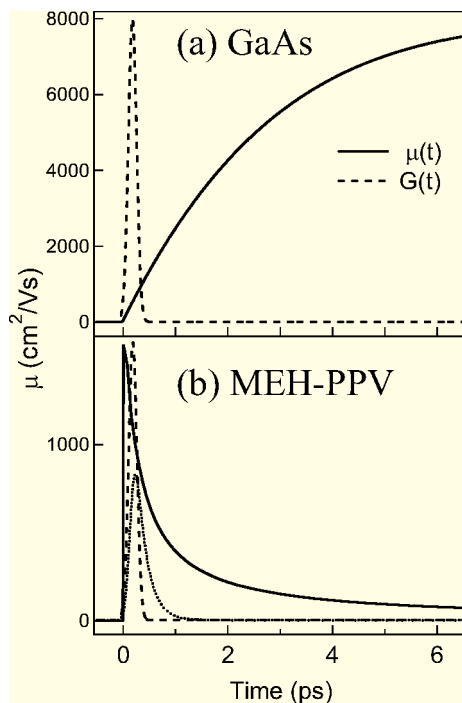


FIG. 2. Comparison of time scales involved in charge generation and cooling; the solid lines in both figures represent the calculated time dependent mobility $\mu(t)$ in (a) GaAs (excitation with 400 nm, calculated using the formalism introduced in Ref. 23) and (b) MEH-PPV (calculated from Ref. 25—see text). Dashed lines represent the generation rate $G(t)$ assuming instantaneous generation of charges upon excitation, i.e., described by the Gaussian intensity profile of the excitation pulse (FWHM 180 fs). The dotted line in (b) describes the generation rate for charges generated from hot excitons with a dissociation rate of $(200 \text{ fs})^{-1}$ (Ref. 29). In (a) the rise in photocurrent is dominated by the slow evolution in $\mu(t)$, while in (b) the rise in $G(t)$ and decay in $\mu(t)$ occur on the same time scale.

The time-dependent mobility of the MEH-PPV sample is calculated following the formalism in Ref. 25. This model is based on the tight-binding approximation combined with static torsional disorder—i.e., deviations from planar alignment of the polymer chain determining its effective conjugation length. The calculated time-dependent diffusivity $D(t)$ is related to the time-dependent mobility in the presence of an applied field through the Einstein relation $\mu(t) = (e/kT)D(t)$.²⁶ The resulting *hole* mobility is plotted in Fig. 2(b). The electron mobility probed in the THz frequency domain is expected to be similar to that of holes. Indeed, microwave conductivity measurements (near 30 GHz) have revealed comparable mobilities of holes and electrons on isolated MEH-PPV chains.²⁷ According to Martens *et al.*,²⁸ the much lower electron mobilities observed in time-of-flight experiments or admittance spectroscopy may be traced to extrinsic effects such as trapping of electrons by impurities or structural defects. On the picosecond time scale involved in the present experiments such extrinsic effects are expected to play a minor role.

Clearly, $\mu(t)$ in MEH-PPV has a shape very different from that in GaAs, with a very large initial value decreasing rapidly towards the small steady state values observed in

these samples [$\sim 10^{-5} \text{ cm}^2/\text{V s}$ (Ref. 22)]. In GaAs, the mobility increases with time as carriers cool and return to the highly mobility state in the Γ valley. In MEH-PPV, the finite conjugation length along the polymer backbone provides a large initial mobility, but greatly restricts charge motion at long times, as the rate determining step at longer times is the hop across the intersegment barrier. This rapid damping of charge motion leads to a maximum in photoconductivity, where the rise in photocurrent is due to the charge generation, and damping by the finite conjugation length causes the subsequent rapid decay. This agrees qualitatively with the double peak structure of the radiated THz field in Fig. 1(b), with the maximum in photocurrent corresponding to the change in sign of the emitted field.

Whereas for GaAs it is apparent that $G(t)$ simply follows the excitation intensity, for the polymer $G(t)$ depends on the precise mechanism of carrier generation. Assuming, however, that $G(t)$ has the same Gaussian profile as the excitation intensity—that is, neglecting any delay in onset of carrier generation (as would be expected from cooling effects or charge generation from exciton-exciton annihilation)—we can reproduce the radiated THz field shown in Fig. 1(b), varying only the amplitude of $G(t)$ as before. The calculated curve reproduces the wave form reasonably well, including the magnitude of positive and negative lobes.

The fact that the calculated radiated field oscillates faster than the measurement suggests that charge generation may not be fully instantaneous, and $G(t)$ may be slightly broader than the intensity profile of the excitation pulse. The dotted line in Fig. 2(b), calculated using a generation rate of $(200 \text{ fs})^{-1}$,²⁹ agrees better with the measured THz pulse in terms of the width, but the agreement in shape is slightly diminished. In any case, this analysis sets an upper limit for charge generation within 200 fs of photoexcitation, which is much faster than the diffusion time scales that would be required for charge generation by, for example, exciton-exciton annihilation⁴ or cold exciton dissociation at defects.³⁰ Hence, another mechanism for rapid charge generation in semiconducting polymers must be operative. It is also evident that the cooling effects observed in GaAs are much less significant in the polymer sample, as these would induce broadening in $\mu(t)$, and a corresponding broadening in the radiated THz field. The good agreement between the calculated and experimentally observed emitted THz field corroborates the theoretical model of dispersive charge transport which is limited by disorder-induced barriers, causing non-Druidian transport.

By comparing the magnitudes of $G(t)$ required to reproduce the data in Fig. 1, and taking into account the excitation fluences used in the experiment, it is straightforward to compare the relative quantum efficiencies of charge generation in the two samples. This yields a quantum efficiency in MEH-PPV of approximately 0.05% of that in GaAs. It should be noted that the accuracy of this number is limited by the accuracy of the model used to describe $\mu(t)$ in the polymer, particularly at short times. On longer time scales (in the ps to ns range), an estimate of this accuracy can be made by comparing mobilities measured in the microwave (30 GHz) region²⁷ to those predicted by the model at the same

frequency.²⁵ From this comparison, it is apparent that the error in the model due to additional nontorsional defects is approximately a factor of 10, though this is certainly much smaller on the subpicosecond time scales, on which the THz radiation is emitted, where defects will play a much less important role. Hence, it is clear that only a small fraction of photoexcitations in the polymer results in the ultrafast generation of free charges. This is inconsistent with the band structure picture, where the initial above band gap photoexcitations initially exist as free charges, which may later relax to subband gap exciton states. In addition, the rapid generation of charge carriers is also not consistent with an exciton-exciton annihilation mechanism, as this requires (slow) exciton diffusion. A more probable mechanism, consistent with both the low quantum efficiency *and* the rapid generation of *thermal* carriers, is through hot exciton dissociation.^{5,6} In this picture unrelaxed, nascent excitons (before cooling) may use the excess excitation energy (above the S_1 ground state) to overcome the dissociation barrier. This may result in a small number of free, thermal charges with a predicted <1% quantum efficiency.^{5,6} An increase in theoretical quantum efficiencies could arise by considering hot exciton dissociation at defects³¹ or from higher lying excited states.³² Since exci-

ton cooling occurs on the 100–300 fs time scale,^{5,6} these mechanisms result in rapid charge generation, entirely consistent with the <200 fs generation time observed in this work.

In conclusion, we have studied charge generation in a semiconducting polymer (MEH-PPV) by measuring the radiated THz wave after photoexciting the polymer with a femtosecond visible pulse in the presence of an electric field. This allows us to study the rise and fall of photocurrents in these materials on subpicosecond time scales. We find an upper limit for charge generation in MEH-PPV of 200 fs after photoexcitation, and estimate the quantum efficiency for charge generation in the polymer to be over two orders of magnitude lower than in GaAs. Both conclusions are consistent with charge generation through hot exciton dissociation in semiconducting polymers.

The authors wish to thank P. C. M. Planken for helpful discussions and R. C. V. van Schie and P. Schakel for excellent technical support. This work was financially supported by the Netherlands Organization for Scientific Research (NWO).

*Electronic address: e.hendry@chem.leidenuniv.nl

¹M. Angelopoulos, IBM J. Res. Dev. **45**, 57 (2001).

²*Conjugated Polymers: Molecular Exciton versus Semiconductor Band Model*, edited by N. S. Sariciftci (World Scientific, Singapore, 1997).

³A. Kohler *et al.*, Nature (London) **392**, 903 (1998). F. A. Hermann *et al.*, Phys. Rev. Lett. **89**, 227403 (2002).

⁴G. J. Denton, N. Tessler, N. T. Harrison, and R. H. Friend, Phys. Rev. Lett. **78**, 733 (1997).

⁵V. I. Arkhipov, E. V. Emelianova, and H. Bässler, Phys. Rev. Lett. **82**, 1321 (1999).

⁶D. M. Basco and E. M. Conwell, Phys. Rev. B **66**, 155210 (2002).

⁷C. H. Lee, G. Yu, and A. J. Heeger, Phys. Rev. B **47**, 15543 (1993).

⁸C. H. Lee, G. Yu, D. Moses, and A. J. Heeger, Phys. Rev. B **49**, 2396 (1994).

⁹D. Moses, H. Okumoto, C. H. Lee, A. J. Heeger, T. Ohnishi, and T. Naguchi, Phys. Rev. B **54**, 4748 (1996).

¹⁰M. C. Beard, G. M. Turner, and C. A. Schmuttenmaer, J. Phys. Chem. B **106**, 7146 (2002).

¹¹E. Hendry, J. N. Schins, L. P. Candeias, L. D. A. Siebbeles, and M. Bonn, Phys. Rev. Lett. **92**, 196601 (2004).

¹²C. Soci and D. Moses, Synth. Met. **139**, 815 (2003).

¹³H. Nemeč *et al.*, J. Appl. Phys. **90**, 1303 (2001).

¹⁴I. H. Campbell, P. S. Davids, D. L. Smith, N. N. Barashkov, and J. P. Ferraris, Appl. Phys. Lett. **72**, 1863 (1998).

¹⁵G. Gallot and D. Grischkowsky, J. Opt. Soc. Am. B **16**, 1204 (1999).

¹⁶Measured laser fluences were corrected for reflection effects using the dielectric functions of GaAs and PPV films, from S. Bergfeld and W. Daum, Phys. Rev. Lett. **90**, 036801 (2003) and

from H. Hoppe, N. S. Sariciftci, and D. Meissner, Mol. Cryst. Liq. Cryst. **385**, 233 (2002), respectively.

¹⁷X. C. Zang, Y. Jin, and X. F. Ma, Appl. Phys. Lett. **61**, 2764 (1992).

¹⁸P. U. Jepsen, R. H. Jacobsen, and S. R. Keiding, J. Opt. Soc. Am. B **13**, 2424 (1996).

¹⁹G. Gallot, J. Zhang, R. W. McGowan, T. I. Jeon, and D. Grischkowsky, Appl. Phys. Lett. **74**, 3450 (1999).

²⁰H. J. Bakker, G. C. Cho, H. Kurz, Q. Wu, and X. C. Zang, J. Opt. Soc. Am. B **15**, 1795 (1998).

²¹J. S. Blakemore, J. Appl. Phys. **53**, R123 (1982).

²²E. Lebedev, T. Dittrich, V. PetrovaKoch, S. Karg, and W. Brütting, Appl. Phys. Lett. **71**, 2686 (1997).

²³C. J. Stanton and D. W. Bailey, Phys. Rev. B **45**, 8369 (1992).

²⁴M. L. Lovejoy, M. R. Melloch, M. S. Lundstrom, and R. K. Ahrenkiel, Appl. Phys. Lett. **61**, 2683 (1992).

²⁵F. C. Grozema, P. T. v. Duijnen, Y. A. Berlin, M. A. Ratner, and L. D. A. Siebbeles, J. Phys. Chem. B **106**, 7791 (2002).

²⁶O. Bénichou and G. Oshanin, Phys. Rev. E **66**, 031101 (2002).

²⁷R. Hoofman, M. P. Haas, L. D. A. Siebbeles, and J. M. Warman, Nature (London) **392**, 54 (1998).

²⁸H. C. F. Martens *et al.*, Appl. Phys. Lett. **77**, 1852 (2000).

²⁹The charge generation rate $G(t)$ now depends on the pump intensity profile $I(t)$, the charge generation rate $k=(200\text{ fs})^{-1}$, and the time-dependent excitation density $N(t)=\int_{-\infty}^t [I(t')-kN(t')]dt'$, such that $G(t)=kN(t)$.

³⁰B. Dulieu, J. Wery, S. Lefrant, and J. Bullo, Phys. Rev. B **57**, 9118 (1998).

³¹D. W. McBranch *et al.*, Synth. Met. **101**, 291 (1999).

³²C. Silva, A. S. Dhoot, D. H. Russell, M. A. Stevens, A. C. Arias, J. D. Mackenzie, N. C. Greenhan, R. H. Friend, S. Setayesh, and K. Nüllen, Phys. Rev. B **64**, 125211 (2001).